MgF_2/CeO_2 AR Coating on p-type (100) Cz Silicon Solar Cells

D. G. Lim*, I. Lee, U. J. Lee, and J. Yi
School of Electrical and Computer Engineering, Sung Kyun Kwan University
300 Chunchun-dong, Jangan-gu, Suwon, Kyunggi-do 440-746, Korea

E-mail : dglim@ece.skku.ac.kr

(Received 27 September 2000, Accepted 21 December 2000)

This paper presents a process optimization of antireflection (AR) coating on crystalline Si solar cells. Theoretical and experimental investigations were performed on a double-layer AR (DLAR) coating of MgF2/CeO2. We investigated CeO2 films as an AR layer because they have a proper refractive index of 2.46 and demonstrate the same lattice constant as Si substrate. RF sputter grown CeO2 film showed deposition temperature strong dependence. The CeO2 film exhibited at 400 °C exhibited a strong (111) preferred orientation and the lowest surface roughness of 6.87 Å. Refractive index of MgF2 film was measured as 1.386 for the most of growth temperature. An optimized DLAR coating showed a reflectance as low as 2.04 % in the wavelengths ranged from 0.4 μm to 1.1 μm. Solar cells with a structure of MgF2/CeO2/Ag/n^+/p-type Si/P^+/Al were investigated with and without DLAR coatings. We achieved the efficiency of solar cells greater than 15 % with 3.12 % improvement with DLAR coatings. Further details about MgF_2, CeO2 films, and cell fabrication parameters are presented in this paper.

Keywords : AR coating, MgF_2, CeO_2, Texturing, Refractive index

1. INTRODUCTION

Struggle thin film solar cells, a single crystalline Si solar cell should be fabricated with a high efficiency and low cost process. In other to increase cell efficiency, there has been a photo-lithographical texturing of Si surface[1]. However, the cell fabrication cost is increased with lithography work, we used a randomly textured Czochralski (Cz) Si wafers. Because reflectance is higher in randomly textured surface than that of lithographically textured one, this paper focused on the effects of anti-reflection coatings. Table 1 shows available materials and their refractive indices (n) for AR coatings. Conventional monolayer AR coating was carried out using SiO2. Many research groups investigated on a double layer AR (DLAR) coating. For a bottom layer of AR coating, the most of investigators used a higher refractive index material in between 2.2 and 2.6. A lower refractive index ranged from 1.3 to 1.6 was employed for a top AR layer. Among the various sets of DLAR coating[2,3], MgF2/ZnS, MgF2/TiO2, and SiO2/SiN have been reported to be the best choice for a minimum reflectance [4-6].

Table 1. Refractive Indices of materials used in single or multiple-layer antireflection coating[2,3].

Materials	Refractive index
Al2O3	1.8~1.9
Galsses	1.5~1.7
MgF2	~1.38
MgO	~1.74
Si3N4	~1.9
SiN	~2.30
SiO	1.8~1.9
SiO2	~1.46
TiO2	~2.30
Ta2O5	2.1~2.3
ZnS	~2.33
CeO	~1.95
CeO2	~2.40
Si	~3.85

This paper studied a DLAR coating with a $MgF_2/CeO_2/Cz$-Si structure. We employed CeO_2 films because it shows a proper refractive index for the bottom AR layer and exhibits the same lattice constant as Si(CeO_2=0.541 nm, Si=0.543 nm). There has been a successful epitaxial Si growth on CeO_2/Si substrate[7-9]. Since surface dangling bonds can be passivated with CeO_2 films, we expect CeO_2 can be very effective in reducing surface state recombination of Si solar cells because CeO_2 film exhibits the same crystalline structure and lattice mismatch about 0.6 % with Si.. Theoretical optimization process and experimental verification were carried out using a DLAR coating of $MgF_2/CeO_2/Cz$-Si.

Fig. 1 shows a structure of the investigated solar cells with DLAR coating layers, Ag top electrode, n+ emitter layer, randomly textured surface, p-type Si base, back surface field, and Al bottom electrode.

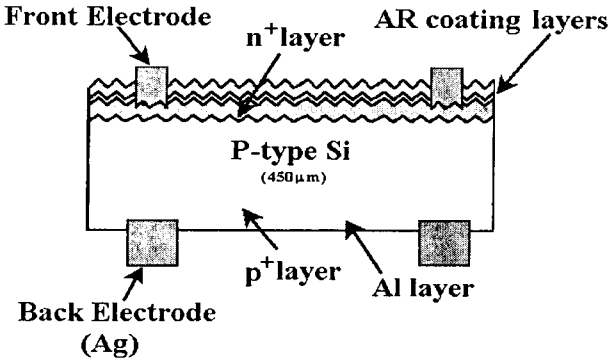

Fig. 1. The structure of investigated Si solar cell.

2. EXPERIMENTAL

We used (100) Cz c-Si wafers grown by LG Siltron with a size of 6-inch, thickness 620 μm resistivity about 5Ω · cm, and minority carrier lifetime 5 μs. Fig. 2 shows experimental procedures followed in our work. Solar cells were fabricated in following orders: Cz wafer cutting, chemical cleaning, Si wafer thinning, randomized texture etching, n-type emitter doping, front side Ag screen printing, backside Al screen printing, IR heat treatment, and DLAR coating. Cz-Si wafers are thinned down to 450 μm thickness to reduce series resistance of a base region. Texturing etch was performed in a mixture of KOH+IPA+DI water where a (100) crystal plane is preferentially attacked and generated pyramid structures. Gaseous diffusion from a liquid $POCl_3$ source was used to make an n-type emitter layer at 880~900 °C for 20 min. To maintain a cost-effective process, we employed a screen printing method for front and backside metallization. Printing Ag paste on a front surface and Al at rear side, the wafers were dried and fired in an infrared belt furnace to form the front contact and back surface field on the wafer. Finally, Ag paste is printed on the back surface, and then this wafer is dried and fired to form the back contact. A diamond saw-cutter (Buehler ISO-9001) was employed to paste p-n junction. Resistivity was measured by a 4-point probe system of Signatone S-30L. Current-Voltage (I-V) characteristics of solar cells were investigated under dark and light illumination. Spectral response was examined using a Jobin Yvon XC-150, MAP23 scanning controller, and Keithley 617.

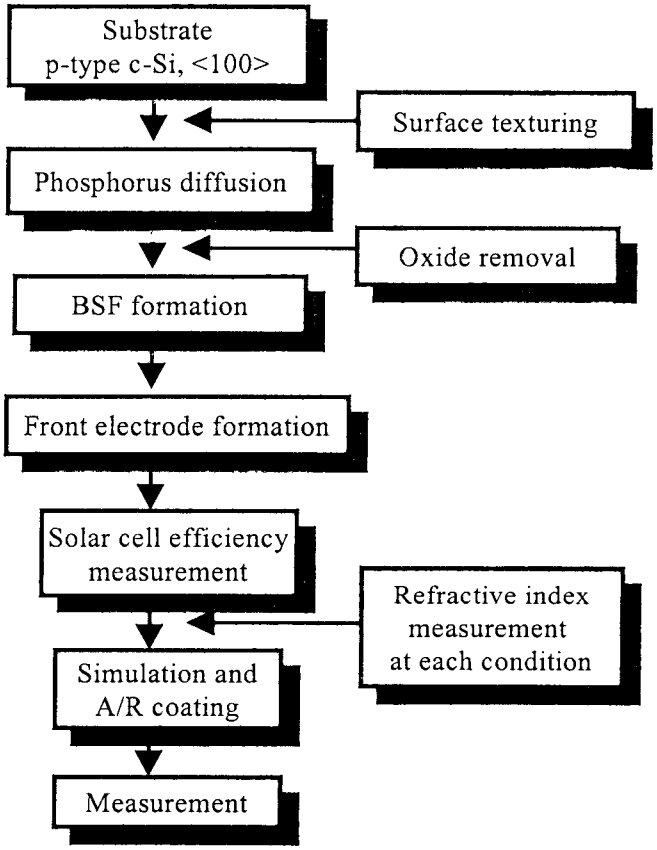

Fig. 2. Experimental procedures.

Small size samples out of 10 cm x 10 cm cells were subjected to AR coating study. CeO_2 thin films were RF sputter deposited using a Ce metallic target with a diameter of 2-inch and 99.9 % purity. The substrate and target were separated by a distance of 5 cm. We changed RF input power from 40 W to 80 W and varied a substrate temperature from RT to 600 °C. The Ar/O_2 gas ratio needs to be controlled very carefully in order to obtain stoichiometric CeO_2 films. We changed gas ratio Ar/O_2 from 5/5 to 9/1 while keeping a total pressure in 20 sccm and 10^{-6} Torr. A substrate temperature was investigated from RT to 400 °C at a step of 100 °C. Piece-type MgF_2 sources (1~4 mm) with purity of

99.999 % were used in the film growth. SEM and AFM (Mitutoyo Auto-probe) examined surface roughness of AR coating layer. Crystallographic properties were characterized using a XRD system of Mac Science M18XHF-SRA with an input power of 40 kV. The XRD scan angle was ranged from 20 to 70 degree with a speed of 8.0 deg./min. Electrical properties of CeO2 and MgF2 films were evaluated by C-V and I-V measurements. Refractive index was measured by an ellipsometer of Gaertner Scientific Cooperation L116B-85B with a wavelength of 6328 Å.

3. RESULTS AND DISCUSSIONS

Crystal structures of the DLAR were investigated for various substrate temperatures. Fig. 3 shows the XRD results on CeO2 and MgF2 films grown at various substrate temperatures. Over the investigated substrate temperatures, CeO2 film structure displayed a (111) preferred orientation. XRD result shows that the CeO2 crystalline peak appears as in crystalline Si peak positions. Having the same lattice constant and crystal structure, we expect to decreases the surface states between CeO2 and Si substrate. We observed a rather weak CeO2 (220) plane with a temperature less than 200 °C. This (220) peak disappeared as the substrate temperature increase higher than 400 °C. RF power dependence of CeO2 suggests that a low power be used for an interface improvements and epi-like CeO2 film growth on Cz Si wafers. Although CeO2 demonstrated crystalline nature at any substrate temperature, MgF2 films were amorphous at RT, and (111) preferred orientation at 100 °C.

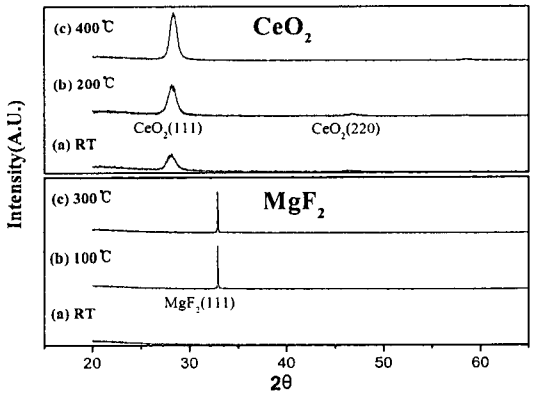

Fig. 3. XRD analysis of CeO2 and MgF2 films for various substrate temperatures.

Fig. 4 shows AFM results on CeO2 films as a function of substrate temperature. Surface roughness was improved 400 °C. Using substrate temperature of 400 °C and Ar/O2 ratio 7/3, we achieved a minimum surface roughness of CeO2 film about 6.87 Å. Considering surface roughness results on CeO2 films, we recommend readers to use a growth temperature of 400 °C, Ar/O2 ratio 7/3, RF power 50 W. Fig. 5 shows the SEM photograph image of MgF2 films. Surface morphology study on MgF2 showed a similar strong dependence on a film growth temperature. Void and pinhole containing MgF2 films were observed for RT grown samples. Surface uniformity was improved with a substrate temperature between 100 °C and 200 °C. However, we monitored enlarged grains and higher surface roughness at a temperature of 300 °C. Surface morphology study on MgF_2 film indicates that a deposition temperature should be kept between 100 ℃ and 200 ℃ for a top layer of DLAR coating.

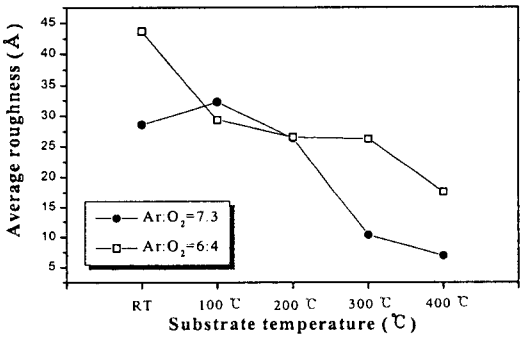

Fig. 4. AFM surface roughness of CeO2 films for different temperatures and Ar/O2 rates.

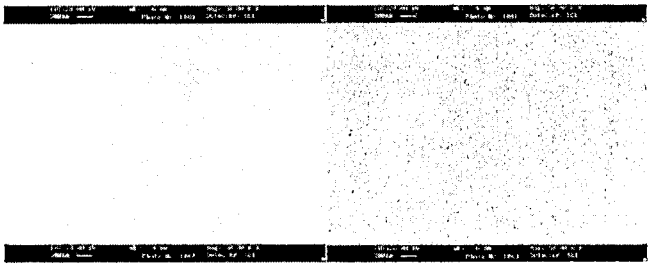

Fig. 5. Surface morphology of MgF2 films as a function of substrate temperature.

XRD and ellipsometer measurement studies on CeO2

films indicated that a film growth temperature is the most important factor for the film property modulations. Refractive index was increased from n=2.352 for RT to n=2.780 for a substrate temperature of 300 °C. For a deposition temperature of 400 °C, however, we observed a reduced refractive index of 2.467. Table 2 lists refractive indices for CeO_2 and MgF_2 with a variation of growth conditions. For a given temperature, CeO_2 films showed an almost constant value of refractive index with the variation of Ar/O_2 gas ratio. The film growth temperature as demonstrated in Table 2 less influenced on a refractive index of MgF_2 films.

Table 2. Refractive Indices of CeO_2 and MgF_2 Films Prepared by Various Conditions.

Material	Variable	Refractive index
CeO_2	T_s = RT	2.352
	T_s = 100 °C	2.702
	T_s = 300 °C	2.780
	T_s = 400 °C	2.467
CeO_2	Ar/ O_2 (9/1)	2.304
	Ar/ O_2 (8/2)	2.228
	Ar/ O_2 (7/3)	2.352
	Ar/ O_2 (6/4)	2.275
	Ar/ O_2 (5/5)	2.334
MgF_2	T_s = RT	1.386
	T_s = 100 °C	1.386
	T_s = 200 °C	1.385

The effect of DLAR coating depended on the refractive index and film thickness of each layer. Ellipsometry study indicated that we can have a control over a refractive index of CeO_2 with the adjustment of growth temperature. We fixed n=1.386 for MgF_2 films because there was very little deviations in a refractive index. To determine the best deposition condition of CeO_2, we carried out simulations on reflectance variations using a measured refractive index and calculated thickness. For the simplicity in reflectance calculation, we considered the imaginary part of refractive index as zero. In theoretical simulations of MgF_2/CeO_2 DLAR coating, we employed a classical optic theory [10]. The optimized thickness of CeO_2 film range from 550 to 650 Å with different n values. Fig. 6 shows the calculated reflectance of DLAR coating with a fixed n=1.38 for MgF_2 and measured refractive index in Table 2 for CeO_2. The CeO_2 deposited at 400 °C shows the lowest average reflectance of $R_{avg.}$=2.04 % in the wavelengths between 0.4 μm to 1.1 μm. The second and third best choice of MgF_2/CeO_2 DLAR coating gave a reflectance equal to Ravg.=2.18 % and Ravg.=2.75 % for RT and 100 °C, respectively. These results lead us to fix the substrate temperature of 400 °C in the deposition of CeO_2. Because SiO_2 layer was formed during $POCl_3$ diffusion, we studied the effect of underlying SiO_2 layer thickness in the reflectance. Fig. 7 shows how the SiO_2 layer thickness influences the total reflectance of solar cells. We can see a little increase of reflectance until SiO_2 thickness reaches to 100 Å. However, as SiO_2 thickness increased above 200 Å, we learn that a reflectance increases to an unacceptable level for solar cell applications.

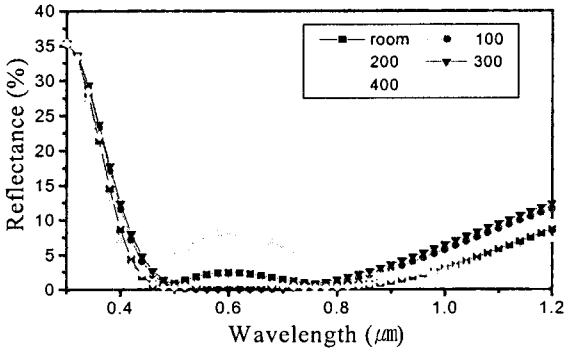

Fig. 6. Reflectance of MgF_2 /CeO_2 /Si DLAR as a function of CeO_2 growth temperature.

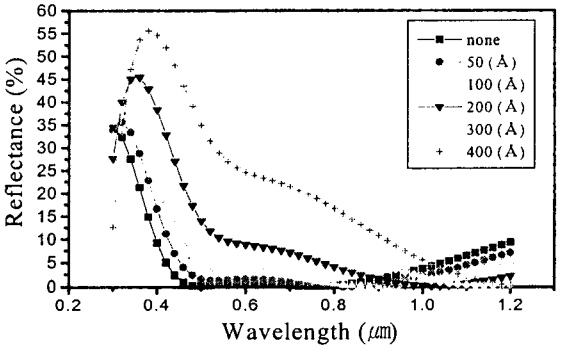

Fig. 7. Thickness on an effect of SiO_2 a reflectance of DLAR coating.

Surface texturing in a solution mixed with $KOH+IPA+H_2O$, $NaOH+IPA+H_2O$, $N_2H_4+H_2O$ gave randomized pyramid structures with a several micron size. From the texturing study, we recommended a slow etching time and frequent change of the chemical solution. If we used solution more than three times, the solution caused stains on Si surface. N-type emitter

junction was formed by careful tailoring of the temperature profile, gas flows rate, and diffusion cycle times. For the sheet resistance about 25 Ω /□ and junction depth about 0.5 ~ 1.0 μm, we obtained the best cell efficiency. The optimized thickness of aluminum paste was in the range of 50± 3 μm. To obtain the good front contact, the contact pattern and the firing condition are properly selected. The best firing temperature were about 770 °C at which the front contact and BSF were formed. The open circuit voltage was decreased with increasing of sheet resistance because of a reduced built-in potential. A small contact area and a sparse line pattern reduced a shadowing loss, but increased a series resistance. Improved cell efficiency was obtained at the ratio of 7.7 % of the grid shading. In AR coating examination, we used small piece type cells taken out of 10 cm x 10 cm cells. Prior to the MgF_2 (n=1.38)/ CeO_2(n=2.467) coating, phosphorous contaminated SiO_2 layer was removed by diluted Schimmel etchant and BHF solutions. For the input power of 20.3 mW/cm^2, L-I-V characteristics were measured. Fig. 8 shows a cell efficiency improvement with a DLAR coating. Current density was improved from 11.67 mA/cm^2 to 15.66 mA/cm^2 giving efficiency improvement of 3.12 %. We suggested this improvement is resulted from the effect of DLAR coating and removal of thin emitter layer.

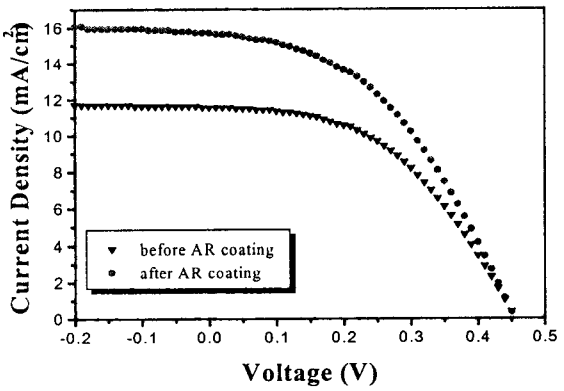

Fig. 8. Solar cell efficiency changes before and after DLAR coating.

4. CONCLUSION

This paper studied an effect of DLAR coatings on randomly textured Cz Si wafers aiming at a low cost and high conversion efficiency of solar cells.

The CeO_2 deposited at 400 °C exhibited the that strong (111) preferred orientation and the lowest surface roughness of 6.87 Å. Optimized refractive indices were given as 1.386 for MgF_2 and 2.407 for CeO_2. We illustrated a MgF_2/CeO_2 coating can reduce reflectance as low as 2.04 % in the wavelength regions of 0.4 ~ 1.1 μm. Reflectance study suggest that thin layer of SiO_2 thickness less than 100 Å does not changed total reflectance of solar cells and safe enough to be used in actual cell fabrications. Solar cells with a structure of $MgF_2/CeO_2/Ag/n^+/p\text{-}Si/P^+/Al$ showed the best characteristics with the BSF formed at 770 °C, grid shading 7.7 %, sheet resistance 25 Ω /□ and junction depth 0.5 μm. Having DLAR coating, we achieved an improvement of 3.2 % for a solar cell efficiency. The further investigations will be directed to increase the active area of DLAR coating, to reduce shading loss with fine grid lines, and to make thin Si base of Cz wafers.

REFERENCES

[1] Martin A. Green, Andrew W. Blakers, Jianhua Zhao, Adele M. Milne, Aihua Wang, and Ximing Dai, *IEEE Trans. Electron Devices*, Vol. 37, No. 2, 1990.

[2] B. J. Thompson, *Thin films for optical systems*, Marcel Dekker Inc., New York, p. 295., 1995.

[3] M. A. Green, *Solar Cells*, Prentice-Hall Inc., New Jersey, p. 164, 1982.

[4] J. Zahao and Martin A. Green, *IEEE Trans. Electron Devices*, Vol. 38, No. 8, 1991.

[5] Zhizhang Chen, Peyman Sana, Jalal Salami, and Ajeet Rohagi, *IEEE Trans. Electron Devices*, Vol. 40, No. 6, 1993.

[6] J. Zahao, Aihua Wang, and Martin A. Green, *IEEE Trans. Electron Devices*, Vol. 41, No. 9, 1994.

[7] Dading Huang, Fuguang Qin, Zhengyu Yao, Zhizhang Ren, and Lanying Lin, *Appl. Phys. Lett.* Vol. 67, No. 25, 1995.

[8] T. Inoue, Y. Yamamoto, S. Koyama, S. Suzuki and Y. Ueda, *Appl. Phys. Lett.*, Vol. 56, No. 14, 1990.

[9] T. Inoue, T. Ohsuna, L. Luo, X. D. Wu, C. J. Maggiore, Y. Yamamoto, Y. Sakurai, and J. H. Chang *Appl. Phys. Lett.*, Vol. 59, No. 27, 1991.

[10] Kasturi Lal Chopra and Sugit Ranjan Das, *Thin Film Solar Cells*, Plenum Press, pp. 515-520, 1983.